

# Reaction Mechanisms of Trp120→Phe and Wild-Type Glucoamylases from *Aspergillus niger*. Interactions with Maltooligodextrins and Acarbose†

Karsten Olsen,† Ulla Christensen,\*‡ Michael R. Sierks,§|| and Birte Svensson\*§

Chemical Laboratory IV, University of Copenhagen, DK-2100 Denmark, and Department of Chemistry, Carlsberg Laboratory, DK-2500 Denmark

Received March 9, 1993; Revised Manuscript Received June 21, 1993\*

**ABSTRACT:** Interactions of wild-type and Trp120→Phe glucoamylase with maltooligodextrin ( $G_x$ ) substrates and the tight-binding inhibitor acarbose (A) were investigated here using stopped-flow fluorescence spectroscopy and steady-state kinetic measurements. All wild-type and Trp120→Phe glucoamylase reactions followed the three-step model  $E + G_x(\text{or } A) (k_1) \rightleftharpoons (k_{-1}) EG_x(\text{or } A) (k_2) \rightleftharpoons (k_{-2}) E^*G_x(\text{or } A) (k_3) \rightarrow E + P \text{ or } E-A$ , previously shown to account for the glucoamylase–maltose system [Olsen, K., Svensson, B., & Christensen, U. (1992) *Eur. J. Biochem.* 209, 777–784].  $K_1 = k_{-1}/k_1$ ,  $k_2$ , and  $k_{-2}$ , and the catalytic constant,  $k_3$ , are determined. Binding of maltooligodextrins in the first reaction step is weak, with little difference between wild-type and Trp120→Phe glucoamylase. The second step, involving a conformational change, in contrast, is strongly influenced by the mutation and by the substrate length. Here wild-type glucoamylase reacts faster and forms more stable intermediates the longer the substrate. In contrast, Trp120→Phe reacts slower the longer the substrate. The effect of the mutation is thus smallest on maltose. The Trp120→Phe substitution reduces the fluorescence signal only by 12–20%, indicating that other tryptophanyl residues are important in reporting the conformational change. Trp120 also strongly influences the actual catalytic step, since the mutation decreases the  $k_c$  values 30–80-fold. Acarbose behaves similar to maltotetraose in the first and the second steps with wild-type but not the Trp120→Phe glucoamylase. Also, a third step in the acarbose reaction which parallels the catalytic step is strongly affected by the mutation. The rate constant  $k_3$  increases 200-fold.

Glucoamylase (1,4- $\alpha$ -D-glucan glucohydrolase, EC 3.2.1.3) catalyzes the release of D-glucose from the nonreducing ends of starch and related oligo- and polysaccharides (Hiromi et al., 1983). Also 1,6- $\alpha$ -D-glucosidic bonds are hydrolyzed but with much lower efficiency (Hiromi et al., 1966a,b). As for many other carbohydrases [for a review, see Svensson and Sogaard (1993)], two catalytic carboxyl groups have been identified (Hiromi et al., 1966a; Svensson et al., 1990; Sierks et al., 1990), and a number of Trp residues have been shown to be involved in interactions with substrates and inhibitors (Hiromi et al., 1983; Clarke & Svensson, 1984a,b; Sierks et al., 1989) leading to a decrease and an increase, respectively, of the intrinsic protein fluorescence of the enzyme.

The insight gained in the past few years into the detailed structure/function relationships in carbohydrases from site-directed mutagenesis studies [for a review, see Svensson and Sogaard (1993)] has mainly come from steady-state kinetics of the mutant enzymes. Moreover, most of the enzymes investigated release the product with retained anomer configuration and thus represent a different version of the mechanism for general acid catalysis of glycosidic bonds than

that of glucoamylase, which catalyzes the release of  $\beta$ -D-glucose [for a review, see Sinnott (1990)]. In most cases the genetic analysis has addressed the catalytic side chains. It was found that mutation of the general acid catalyst leads to a very great loss in  $k_{cat}$ , while mutant enzymes of considerable residual activity (0.01–2%) resulted from replacements of the general base catalyst. A very important group of starch hydrolases, the  $\alpha$ -amylases (Nagashima et al., 1992) and their related enzymes with different substrate specificity, such as for example the neopollulanase (Kuriki et al., 1991) and cyclodextrin glucanotransferase (Nakamura et al., 1992), show no detectable activity after mutation of any of the catalytic carboxylic acid residues. In contrast, the *Aspergillus niger* glucoamylase shows 0.05% residual activity against maltoheptaose after mutation of the general acid catalyst Glu179 to Gln (Sierks et al., 1990). The general base catalyst was identified recently by X-ray crystallography (Harris et al., 1993) and a corresponding mutant, Glu400→Gln, showed 2% of the wild-type activity against maltoheptaose (Frandsen et al., 1993). In contrast to the majority of starch hydrolases, glucoamylase thus allows studies on the effect of mutations at the catalytic groups.

Like many glycosidases, glucoamylase from *A. niger* is strongly inhibited by hexose derivatives and oligosaccharide structural analogues with an NH group adjacent to C-1. Acarbose (Figure 1) is a pseudotetrasaccharide from this group of inhibitory compounds and was early acknowledged as a strong inhibitor of fungal glucoamylase (Truscheit et al., 1981). It remains an open question, however, to which extent the planar conformation at the valienamine ring and the protonated cationic nitrogen ( $pK_a$  approximately 5) in the pseudoglycoside bond contribute to the inhibitory strength. The binding mechanism of acarbose is unknown; binding studies with structurally related compounds, however, indicated that the

† This work was supported by the Danish Technology Council (Grant 1990-133/443-900088), by the Danish Science Research Council [Grants 11-6876 and 11-7542 (U.C.)], and by the Carlsberg Foundation [Grants 88-0093/40 and 80-0098/10 (U.C.)].

\* Address correspondence to this author at Chemical Laboratory IV, Universitetsparken 5, DK-2100 Copenhagen, Denmark (U.C.) or Department of Chemistry, Carlsberg Laboratory, DK-2500 Valby, Denmark (B.S.).

‡ University of Copenhagen.

§ Carlsberg Laboratory.

|| Present address: Department of Chemical and Biochemical Engineering, University of Maryland, Baltimore County, Baltimore, MD 21228.

\* Abstract published in *Advance ACS Abstracts*, August 15, 1993.

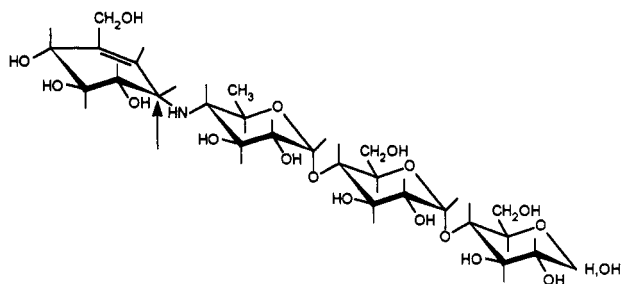
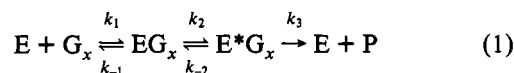


FIGURE 1: Structural formula for acarbose. The arrow indicates C-1.

conformation of the valienamine ring and the length of the oligosaccharide were important for the inhibition (Svensson & Sierks, 1992). In the light of the extensive use of this type and related substrate analogues in inhibition studies also of more sophisticated systems such as biosynthesis and trimming of glycoconjugates, advantage was here taken of the access to comfortable amounts of glucoamylase and specific glucoamylase mutants to compare the binding kinetics of acarbose and oligodextrin substrates.

In *A. niger* glucoamylase, one of the functionally very important residues is Trp120, which is invariantly occurring in fungal glucoamylases (Itoh et al., 1987). It is protected against *N*-bromosuccinimide oxidation by acarbose and by the substrate maltotetraose, but to a lesser extent (Savel'ev & Firsov, 1983). It has been concluded that Trp120 is important for (i) communication between substrate glucosyl residue association at subsites 2 and 4, (ii) transition state stabilization, and (iii) the bond-type specificity (Clarke & Svensson, 1984a,b; Sierks et al., 1989; Svensson & Sierks, 1992). In the light of the recent results of the structure/function relationships investigations in the glucoamylase from *A. niger* employing chemical modifications in conjunction with mutagenesis (Clarke & Svensson, 1984b; Sierks et al., 1989, 1990; Svensson et al., 1990), we have undertaken pre-steady-state kinetic studies of the reactions of the enzyme and the Trp120→Phe mutant. A reaction model (eq 1) for the formation of the enzyme-substrate intermediate of which the conversion is rate determining,  $E^*G_x$ , i.e., the intermediate preceding the transition state of the actual catalytic step, has been shown to account for the glucoamylases from *A. niger* (Olsen et al., 1992) and from *Rhizopus niveus* (Tanaka et al., 1982).



The corresponding steady-state kinetic parameters are

$$K_m = \frac{k_{-1}(k_{-2} + k_3) + k_2k_3}{k_1(k_{-2} + k_2 + k_3)} \quad (2)$$

and

$$k_c = \frac{k_2k_3}{k_{-2} + k_2 + k_3} \quad (3)$$

where  $K_m$  and  $k_c$  are the regular kinetic parameters of the Michaelis-Menten equation.

In the present study we report pre-steady-state and steady-state kinetic and thermodynamic results on the interactions of the wild-type and the Trp120→Phe mutant glucoamylase from *A. niger* with the tight-binding inhibitor acarbose (A) and the maltooligodextrin series ( $G_x$ ), maltose to maltopentaose. The analysis implicates Trp120 in the rearrangement  $EG_x \rightleftharpoons E^*G_x$ , the formation of the final E-A complex, and

in transition state stabilization of the catalytic step of substrate hydrolysis. The new details are in accordance with the overall roles assigned previously to Trp120 in the ligand complexation at the fourth subsite (Clarke & Svensson, 1984a,b) and in the transition state stabilization (Sierks et al., 1989). Moreover, NE1 or Trp120 was seen in the three-dimensional structure to hydrogen-bond with OE2 of Glu179, the general acid catalyst (Aleshin et al., 1992).

## MATERIALS AND METHODS

**Materials.** Glucoamylase G1 from *A. niger* was purified from AMG 200 (Novo Industries, Bagsvaerd, Denmark) essentially as described by Svensson et al. (1982). The Trp120→Phe glucoamylase mutant gene (Sierks et al., 1989) was expressed in *A. niger*, and the mutant enzyme was isolated from the culture supernatant (obtained from Drs. Jan Lehmbeck and Frank Andersen, Novo Nordisk, Bagsvaerd) after diafiltration, affinity chromatography on acarbose-Sepharose (Clarke & Svensson, 1984b), and purification of the G1 form of 616 amino acid residues (Svensson et al., 1983) by FPLC-chromatography on a High Load Q-Sepharose essentially as described recently (Stoffer et al., 1993). Protein concentration was determined spectrophotometrically at 280 nm using  $\epsilon_M = 1.37 \times 10^5 \text{ M}^{-1}\text{cm}^{-1}$  (Clarke & Svensson, 1984a) and  $\epsilon_M = 1.31 \times 10^5 \text{ M}^{-1}\text{cm}^{-1}$  for the wild-type and Trp120→Phe glucoamylase G1, respectively. Maltose, maltotetraose, and maltopentaose were obtained from Merck (Darmstadt, Germany), and maltotriose was obtained from Aldrich (Steinheim, Germany). The D-glucose oxidase kit for determination of glucose was purchased from Sigma Chemical Co. (St. Louis, MO). Acarbose (Bay g 5412) was a gift from Drs. D. Schmidt and E. Truscheit (Bayer AG, Germany).

**Stopped-Flow Fluorescence Kinetics.** The pre-steady-state kinetics of the binding of ligands to glucoamylase was followed by measuring the changes of the intrinsic protein fluorescence intensity essentially as described by Olsen et al. (1992). Experiments were performed in a Hi-Tech Scientific PQ/SF-53 spectrofluorometer equipped with a high-intensity xenon arc lamp. The excitation wavelength was 280 nm, slit width 5 nm. Light emitted from the reaction mixture was monitored after passage of a cut-off emission filter (WG 320; 80% transmittance at 320 nm). In this way an integrated emission signal is obtained. A series of stopped-flow experiments were performed at 8 °C in 0.05 M acetate buffer, pH 4.5. After rapid mixing of enzyme (6.5  $\mu\text{M}$  and 3.4  $\mu\text{M}$  for the wild-type and Trp120→Phe glucoamylase G1, respectively, final concentration) and the appropriate ligand solution, the time course of the intrinsic fluorescence intensity (arbitrary units, V) was recorded. Mixing was achieved in less than 1 ms. In each experiment 400 pairs of data were recorded, and generally sets of data from four experiments were averaged. Each averaged set of stopped-flow data were then fitted to a number of nonlinear analytical equations using the Hi-Tech HS-1 Data Pro software. The regression analysis used is based on the Gauss-Newton procedure.

**Steady-State Kinetic Analysis.** The hydrolysis of maltooligodextrins was performed in 0.05 M sodium acetate, pH 4.5, at 8 °C using 8–12 substrate concentrations in the ranges: maltose,  $7 \times 10^{-6}$  to  $8 \times 10^{-4}$  M (at  $1.02 \times 10^{-8}$  M of wild-type and  $4.22 \times 10^{-7}$  M of Trp120→Phe glucoamylase); maltotriose,  $5 \times 10^{-6}$  to  $3 \times 10^{-4}$  M (at  $1.73 \times 10^{-8}$  M of wild-type and  $4.22 \times 10^{-7}$  M of Trp120→Phe); maltotetraose,  $4 \times 10^{-6}$  to  $4 \times 10^{-4}$  M (at  $1.17 \times 10^{-8}$  M of wild-type and  $2.13 \times 10^{-7}$  M of Trp120→Phe); maltopentaose,  $1.5 \times 10^{-5}$

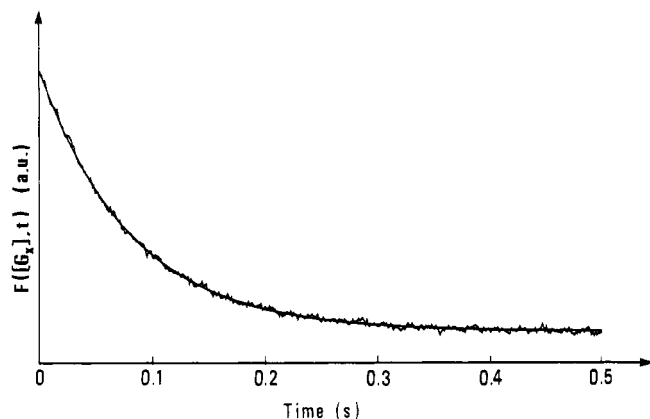


FIGURE 2: Typical time course of the intrinsic protein fluorescence intensity decrease caused by the binding of maltotetraose to the Trp120→Phe mutant glucoamylase. Excitation wavelength was 280 nm. The signal represents the total fluorescence emission above 320 nm. The final concentrations were 3.4  $\mu$ M Trp120→Phe glucoamylase and 0.16 mM maltotetraose, pH 4.5, 8 °C. The fitted curve corresponds to an overall first-order progress (eq 4).

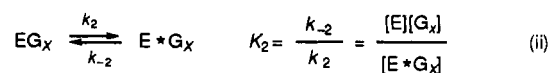
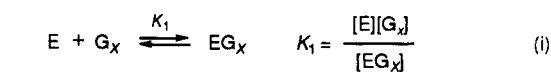
to  $5 \times 10^{-4}$  M (at  $1.17 \times 10^{-8}$  M of wild-type and  $4.22 \times 10^{-7}$  M of Trp120→Phe). Each initial rate was based on 7–10 points of the progress curve of the reaction. The aliquots removed were quenched and assayed as previously reported by the glucose oxidase method (Fleming & Pegler, 1963), transferred to a microtiter plate, and the absorbances measured using a ELISA reader (Fox & Robyt, 1991).

**Analysis of the Data.** The kinetic parameters were determined from fits of the appropriate equations to the data using the nonlinear least-squares fitting program GraFit (Erithacus Software Ltd.) or Enzfitter (Elsevier-BIOSOFT).

## RESULTS

**Binding of Ligands to Glucoamylase.** Typical stopped-flow traces of the binding of substrates to the wild-type and

### Scheme I



Trp120→Phe glucoamylase, as illustrated in Figure 2 show only one relaxation, and the fitted curves correspond to a single-exponential progress:

$$\Delta F([G_x], t) = \Delta F([G_x], \infty)(1 - \exp(-k_{\text{obs}}t)) \quad (4)$$

where  $k_{\text{obs}}$  (general precision;  $\pm 3\%$ ) is the observed first-order rate constant, and  $\Delta F([G_x], t)$  (general precision,  $\pm 1\%$ ) is the relative fluorescence change observed at the actual ligand concentration,  $[G_x]$ , and time,  $t$ . The value  $\Delta F([G_x], \infty)$  is attained at equilibrium of this initial binding at a time,  $t$ , where no (or only negligible) hydrolysis has yet occurred. Equation 4 describes the most accurate fit to the measured data at all concentrations of all ligands employed.

**Maltooligodextrin Substrates.** The dependencies of the observed first-order rate constant,  $k_{\text{obs}}$  (eq 4) on the concentration,  $[G_x]$ , of maltooligodextrin substrate for the wild-type and the Trp120→Phe mutant are shown in Figure 3, A and B, respectively. The hyperbolic behavior of  $k_{\text{obs}}$  on  $[G_x]$  is consistent with the two-step mechanism shown in Scheme I (i and ii) and rules out a simple one-step binding mechanism as represented in Scheme I(i), which requires a linear dependence, i.e.,  $k_{\text{obs}} = k_1[G_x] + k_{-1}$ .

Scheme I involves a fast association of enzyme, E, and substrate,  $G_x$ , followed by a slow change of the conformation of the first association complex,  $EG_x$ , giving rise to the fluorescence change, which is indicated by an asterisk (\*). The corresponding expressions of the substrate concentration dependencies of  $k_{\text{obs}}$  and of  $\Delta F([G_x], \infty)$  (eq 4) are given in

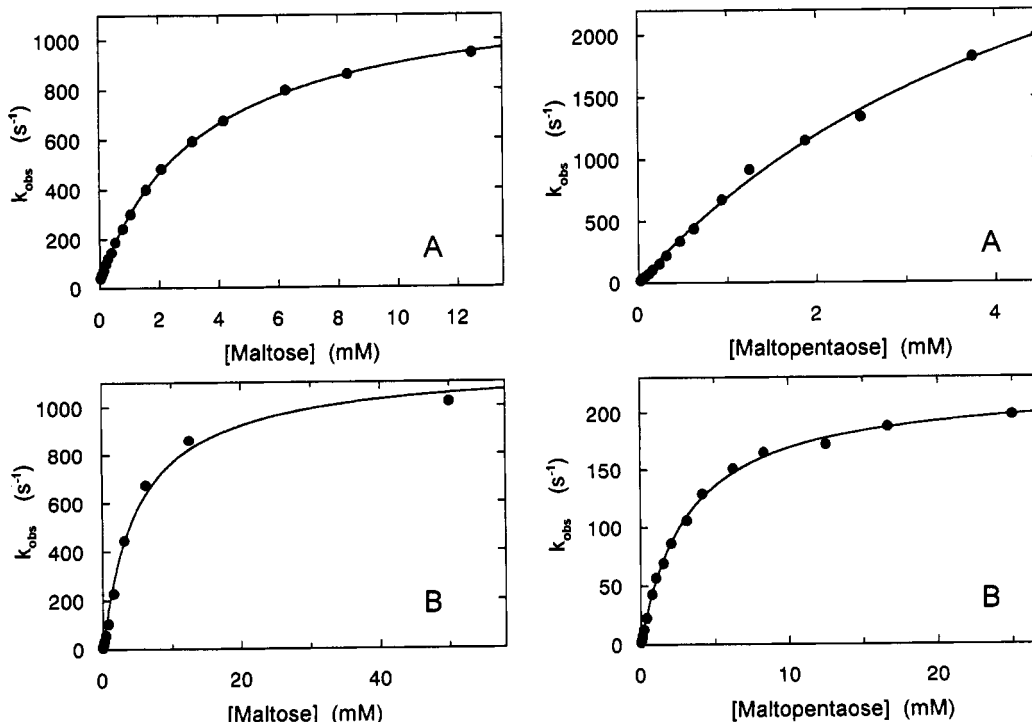


FIGURE 3: Dependencies of the observed rate constant,  $k_{\text{obs}}$  (eq 4), on the concentration of two of the maltooligodextrin substrates. All substrates showed similar results. (A) Wild-type glucoamylase and (B) Trp120→Phe mutant glucoamylase. The lines shown are those obtained from fitting eq 5 to the data. Experimental conditions: pH 4.5, 8 °C, (A) 6.5  $\mu$ M wild-type, and (B) 3.4  $\mu$ M mutant glucoamylase. Relative standard deviation:  $\pm 3\%$ .

Table I: Kinetic Results of the Binding of Ligands to Wild-Type Glucoamylase (pH 4.5, 8 °C)

ligand	$K_1$ ( $\mu\text{M}$ )	$k_2$ ( $\text{s}^{-1}$ )	$k_{-2}$ ( $\text{s}^{-1}$ )	$\Delta F_{\max}(G_x, \infty)$ (%)	$K_d$ ( $\mu\text{M}$ )	$K_m$ ( $\mu\text{M}$ )	$k_c$ ( $\text{s}^{-1}$ )
maltose	$3400 \pm 100$	$1170 \pm 10$	$33 \pm 1$	$19.7 \pm 0.2$	$270 \pm 10^a$ $100 \pm 10^b$	$180 \pm 20$	$0.33 \pm 0.01$
maltotriose	$2000 \pm 100$	$1630 \pm 20$	$23 \pm 1$	$19.5 \pm 0.2$	$53 \pm 2^a$ $28 \pm 2^b$	$57 \pm 6$	$1.75 \pm 0.05$
maltotetraose	$2500 \pm 100$	$2300 \pm 70$	$13 \pm 1$	$17.5 \pm 0.2$	$20 \pm 2^a$ $14 \pm 1^b$	$32 \pm 6$	$3.20 \pm 0.20$
maltopentaose	$5400 \pm 600$	$4400 \pm 350$	$8.5 \pm 0.1$	$15.5 \pm 0.2$	$16 \pm 1^a$ $10 \pm 2^b$	$22 \pm 4$	$4.40 \pm 0.20$
acarbose	$15000 \pm 1500$	$2500 \pm 200$	$2.4 \pm 0.2$	$17.3 \pm 0.3$	$19 \pm 2^a$ $14 \pm 2^b$		

<sup>a</sup>  $K_d$  as calculated from the equilibrium values of the  $\Delta F([G_x], \infty)$ . <sup>b</sup>  $K_d$  as calculated according to  $K_d = K_1 K_2$ .

Table II: Kinetic Results of the Binding of Ligands to W120F Mutant Glucoamylase (pH 4.5, 8 °C)

ligand	$K_1$ ( $\mu\text{M}$ )	$k_2$ ( $\text{s}^{-1}$ )	$k_{-2}$ ( $\text{s}^{-1}$ )	$\Delta F_{\max}(G_x, \infty)$ (%)	$K_d$ ( $\mu\text{M}$ )	$K_m$ ( $\mu\text{M}$ )	$k_c$ ( $\text{s}^{-1}$ )
maltose	$5200 \pm 500$	$1150 \pm 30$	$4.3 \pm 0.5$	$17.5 \pm 0.4$	$45 \pm 5^a$ $20 \pm 3^b$	$52 \pm 3$	$0.01 \pm 0.0002$
maltotriose	$7000 \pm 300$	$770 \pm 15$	$2.2 \pm 0.2$	$15.5 \pm 0.2$	$14 \pm 2^a$ $20 \pm 2^b$	$44 \pm 5$	$0.034 \pm 0.001$
maltotetraose	$4500 \pm 300$	$350 \pm 15$	$0.4 \pm 0.04$	$13.3 \pm 0.2$	$7 \pm 0.3^a$ $5 \pm 0.6^b$	$32 \pm 7$	$0.058 \pm 0.003$
maltopentaose	$3300 \pm 100$	$225 \pm 10$	$0.3 \pm 0.03$	$13.0 \pm 0.2$	$5 \pm 0.3^a$ $4.4 \pm 0.5^b$	$24 \pm 6$	$0.052 \pm 0.004$
acarbose		$\sim 750$		$\sim 13$			

<sup>a</sup>  $K_d$  as calculated from the equilibrium values of the  $\Delta F([G_x], \infty)$ . <sup>b</sup>  $K_d$  as calculated according to  $K_d = K_1 K_2$ .

eqs 5 and 6 (Cherlinski, 1966):

$$k_{\text{obs}} = \frac{k_2}{1 + \frac{K_1}{[G_x]}} + k_{-2} \quad (5)$$

$$\Delta F([G_x], \infty) = \frac{\Delta F_{\max}(G_x, \infty)}{1 + \frac{K_1 K_2}{[G_x](1 + K_2)}} \quad (6)$$

where  $\Delta F_{\max}(G_x, \infty)$  is the maximum relative fluorescence change at saturating concentration of substrate. After obtaining  $k_{-2}$  as the ordinate intercept from a linear extrapolation in the low concentration range, eq 5 was fitted to the data. The resultant values of  $K_1$ ,  $k_2$ , and  $k_{-2}$  thus determined for the pre-steady-state binding of maltooligodextrins to wild-type and Trp120→Phe glucoamylase (Figure 3A,B) are given in Tables I and II.  $K_d$  is the overall dissociation constant, which for  $k_{-2} \ll k_2$  according to Scheme I becomes

$$K_d = \frac{[E][G_x]}{[EG_x] + [E^*G_x]} = \frac{K_1}{1 + k_2/k_{-2}} = \frac{K_1 K_2}{1 + K_2} \simeq K_1 K_2 \quad (7)$$

Tables I and II also list values of  $\Delta F_{\max}(G_x, \infty)$  and  $K_d$  obtained from fits to eq 6 of the equilibrium values of the fluorescence intensity decrease,  $\Delta F([G_x], \infty)$ , of wild-type (Figure 4A) and Trp120→Phe glucoamylase (Figure 4B) and the steady-state kinetic parameters,  $K_m$  and  $k_{\text{cat}}$ , obtained for hydrolysis of the maltooligodextrins catalyzed by the wild-type and Trp120→Phe glucoamylase.

**Acarbose.** Two phases giving rise to opposite changes of the intrinsic fluorescence were discerned when acarbose was reacted with either wild-type or Trp120→Phe glucoamylase. Of the wild-type enzyme the two phases were clearly time-resolved, and the first phase observed (Figure 5 and Table I) closely resembles that observed with the maltooligodextrin substrates. A similar detailed analysis of the reaction with the Trp120→Phe mutant is not possible because of overlap with the second phase of the reaction. But as is illustrated

in Figure 6 approximate values of  $k_{\text{obs}}$  and of  $\Delta F([A], \infty)$  (eq 4), obtained from the original curves strongly indicate that also the substrate and acarbose reactions of the mutant are similar in the first phase (Table II).

Figure 7 shows the concentration dependencies of the observed first-order rate constants of the second phase of the acarbose–glucoamylase reactions that result in fluorescence increases (Clarke & Svensson, 1984a). Whereas the first phase is in accordance with that observed for the substrates, the second phase is unique for acarbose and represents a third reaction step, which may be the final step in the formation of the tightly bound acarbose–enzyme complex.

The hyperbolic dependence of the first-order rate constant,  $k_{\text{obs},2}$ , on the concentration of acarbose,  $[A]$  (Figure 7), is consistent with the three-step mechanism shown in eq 1. When it is assumed that steady state prevails in the first and second reaction steps, the kinetic parameters,  $K_d'$  and  $k'$ , for the second phase of the acarbose reaction are expressed similarly to those of eqs 2 and 3, so that in accordance with Figure 7,  $k_{\text{obs},2}$  becomes

$$k_{\text{obs},2} = \frac{k'}{1 + \frac{K_d'}{[A]}} \quad (8)$$

The results of the analysis according to eq 8 are given in Table III. The corresponding acarbose concentration dependency of  $\Delta F_2([A], \infty)$  is

$$\Delta F_2([A], \infty) = \frac{\Delta F_{\max,2}(A, \infty)}{1 + \frac{K_1 K_2 K_3}{[A](1 + K_3 + K_2 K_3)}} \quad (9)$$

However, if saturating conditions prevail ( $[A] \gg K_1 = K_1 K_2 K_3 / (1 + K_3 + K_2 K_3)$ ) as in our experiments, no concentration dependency of  $\Delta F_2([A], \infty)$  is observed.

## DISCUSSION

The pre-steady-state kinetics of the hydrolysis of a series of oligomer substrates catalyzed by the wild-type and the

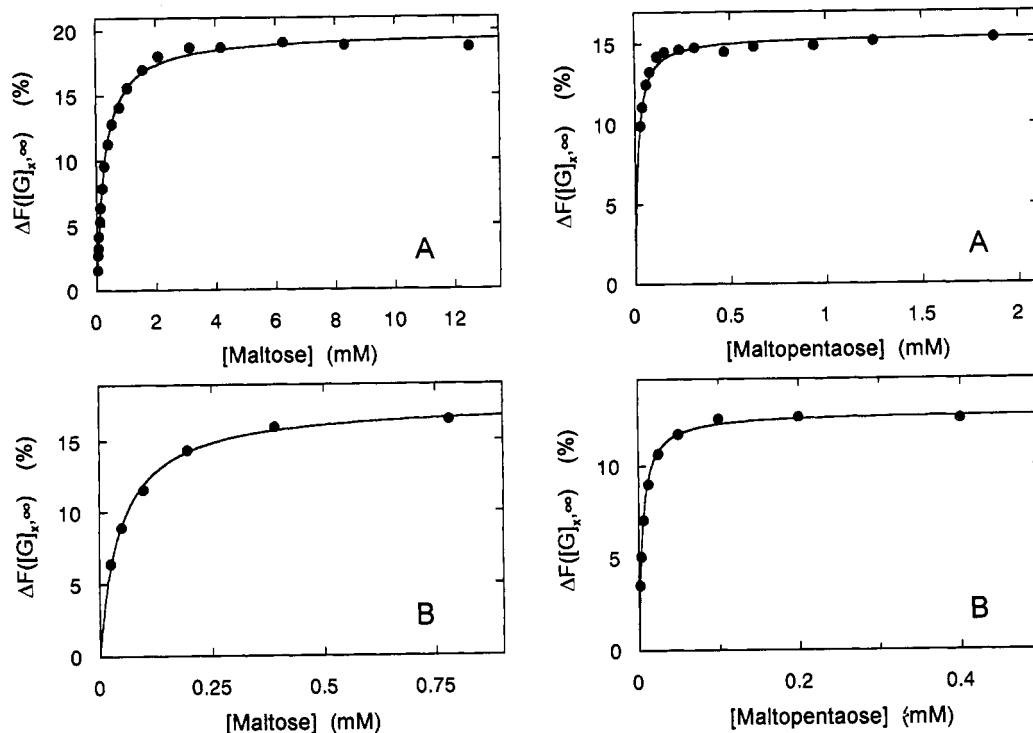


FIGURE 4: Pre-steady-state equilibrium values of the relative fluorescence intensity decrease,  $\Delta F([G]_x, \infty)$  (eq 4), obtained after binding of maltooligodextrin plotted against the concentration of two of the maltooligodextrins. (A) Wild-type glucoamylase and (B) Trp120→Phe mutant glucoamylase. The lines shown are those obtained from fitting eq 6 to the data.  $\Delta F([G]_x, \infty)$  values were obtained at reaction times at which no hydrolysis was yet observed. Experimental conditions: pH 4.5, 8 °C, (A) 6.5  $\mu$ M wild-type, and (B) 3.4  $\mu$ M mutant glucoamylase (maltose); 0.2  $\mu$ M (maltopentaose). Relative standard deviation:  $\pm 1\%$ .

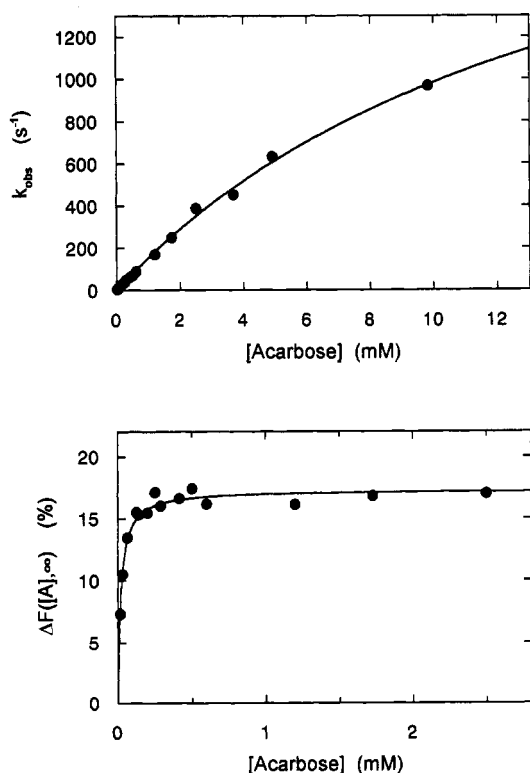


FIGURE 5: Wild-type glucoamylase–acarbose, [A], interaction. Dependencies of the observed rate constant,  $k_{obs}$ , and  $\Delta F([A]_x, \infty)$  on the concentration of acarbose. The lines shown are those obtained from fitting eqs 5 and 6, respectively, to the data. Experimental conditions: pH 4.5, 8 °C, 6.5  $\mu$ M enzyme. Relative standard deviations:  $k_{obs}$  data ( $\pm 3\%$ ) and  $\Delta F([A]_x, \infty)$  data ( $\pm 2\%$ ).

Trp120→Phe mutant of glucoamylase from *A. niger* were studied using stopped-flow fluorescence measurements. In previous pre-steady-state kinetic analysis of *Rhizopus* glu-

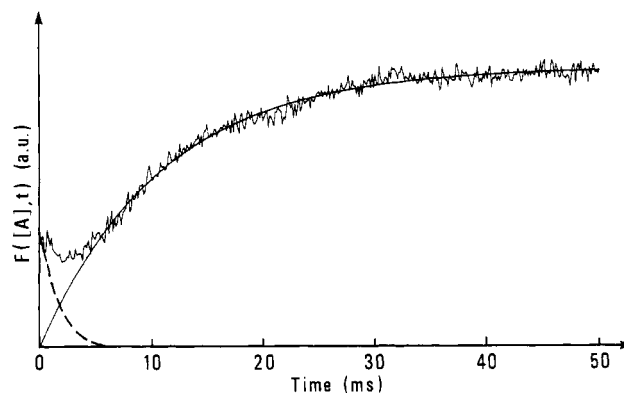


FIGURE 6: Trp120→Phe mutant glucoamylase–acarbose [A] interaction. A characteristic time course experiment is shown. The upper curve was obtained from a fit of eq 4, which provided the values of  $k_{obs,2}$  and  $\Delta F_2([A]_x, \infty)$  for  $[A] = 7.5$  mM, the actual value of the acarbose concentration. The lower curve, which corresponds with the first phase of the reaction, was obtained by subtraction. Experimental conditions: 3.2  $\mu$ M Trp120→Phe mutant glucoamylase and 7.5 mM acarbose, pH 4.5, 8 °C.

coamylase, as well as in the present study, equilibrium mixtures of the  $\beta$ - and  $\alpha$ -anomeric forms of the substrates have been used (Hiromi et al., 1983), with an assumed  $\alpha:\beta$  ratio of 4:6 of the ultimate glucose unit (the reducing end of the substrate). If an effect of different anomer configuration in the binding mechanism exists, it must be expected to decrease with increasing size of the substrate. The concentration dependencies of the observed rates and changes of fluorescence intensity of these processes (Figures 3A,B and 4A,B) correspond with a two-step reaction model (Scheme I) in which initial fast association of the substrate is followed by a conformational change of the enzyme–substrate complexes in a rather fast step, but with measurable rates. The deducible equilibrium and rate constants of the processes ( $K_1$  and  $k_2$ , and  $k_{-2}$ ) are given in Tables I and II together with the steady-

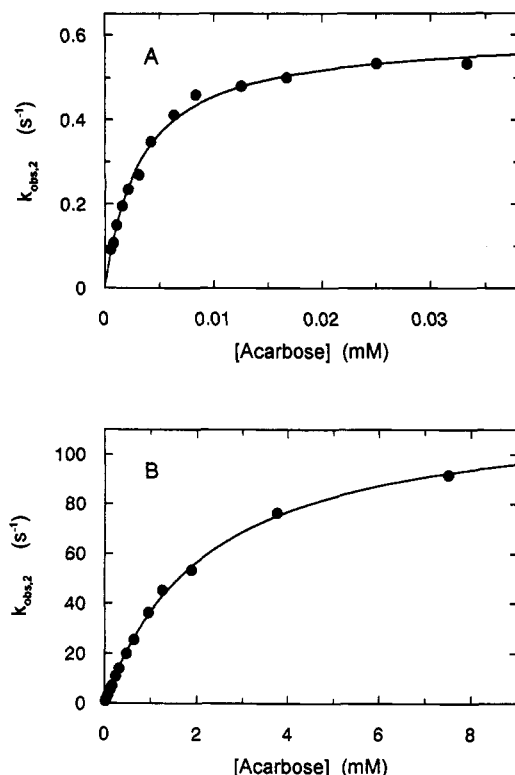


FIGURE 7: Dependencies on the concentration of acarbose,  $[A]$ , of the observed first-order rate constant,  $k_{\text{obs},2}$ , of the second phase of the acarbose-enzyme interactions. (A) Wild-type glucoamylase and (B) Trp120→Phe mutant glucoamylase. The lines shown are those obtained from fitting eq 8 to the data. In the reaction with the mutant,  $k_3$  is obtained from  $k' = k_2 k_3 / (k_2 + k_3)$  (eq 3). With  $k' = 120 \text{ s}^{-1}$ ,  $k_3$  becomes  $\approx 140 \text{ s}^{-1}$ . Experimental conditions: pH 4.5, 8 °C, (A) 0.1  $\mu\text{M}$  wild-type, and (B) 3.2  $\mu\text{M}$  mutant glucoamylase. Relative standard deviation: (A) wild-type ( $\pm 3\%$ ) and mutant glucoamylase ( $\pm 5\%$ ).

Table III: Kinetic Results of the Binding of Acarbose to Wild-Type and Trp120→Phe Mutant Glucoamylase (pH 4.5, 8 °C)

enzyme	$K_d'$ (M)	$k_3$ ( $\text{s}^{-1}$ )	$k_{-3}$ ( $\text{s}^{-1}$ )	$K_1$ (M)
wild-type	$(3.0 \pm 0.2) \times 10^{-6}$	$0.6 \pm 0.01$	$\leq 0.01$	$< 6 \times 10^{-12}$ <sup>a</sup>
Trp120→Phe	$(2.2 \pm 0.1) \times 10^{-3}$	$\sim 140$	$\leq 0.1$	$< 2 \times 10^{-6}$

<sup>a</sup> From Svensson and Sierks (1992) at 25 °C.

state kinetic parameters ( $k_c$  and  $K_m$ ). Because  $k_c \ll k_2$ , and  $k_{-2} \ll k_2$ , eq 3 becomes

$$k_c = \frac{k_2 k_3}{k_{-2} + k_2 + k_3} \approx k_3 \quad (12)$$

The rate-determining step of glucoamylase catalyzed hydrolysis of the substrates thus is preceded by (at least) two steps.

Equation 2 is reduced similarly to give

$$K_m = \frac{k_{-1}(k_{-2} + k_3) + k_2 k_3}{k_1(k_{-2} + k_2 + k_3)} \approx K_1 K_2 = K_d \quad (13)$$

As seen in Tables I and II, the values of  $K_d$  and  $K_m$  of each maltooligodextrin obtained on the wild-type enzyme in pre-steady-state and steady-state experiments, respectively, are indeed of the same order of magnitude.

For an extended mechanism containing more steps than that of eq 1, the resulting  $K_m$  value would be less than that of  $K_1 K_2$  (viz.  $K_m/[G_x] = [E]/\sum_i [EG_x]_i$ , where  $\sum_i [EG_x]_i$  is the sum of all the bound enzyme species, whereas  $K_1 K_2/[G_x] = [E]/[E^*G_x]$ ). We therefore conclude that the reaction mechanism of hydrolysis of all the substrates is one in which

the rate-determining step of the process follows directly after the two steps observed in the stopped-flow experiments as previously shown for maltose (Olsen et al., 1992).

It is obvious from the results (Tables I and II) that the first association step of the wild-type enzyme, as well as of the Trp120→Phe mutant enzyme with each of the substrates is weak ( $K_1$  values are in the millimolar range) compared to the binding forces of the second enzyme-substrate intermediate ( $K_1 K_2 < K_1$ ). Little or no effect of substrate length was seen in  $K_1$ . The first association step then apparently does not discriminate between the oligosaccharides, and thus probably even less between the  $\beta$ - and  $\alpha$ -anomers of the substrates. That structural detail of the substrate apparently is of little importance. This is, further, in accordance with steady-state experiments on methyl  $\beta$ -D-maltoside, which is hydrolyzed by the *A. niger* glucoamylase with essentially the same specificity constant as is maltose (Sierks & Svensson, 1992).

With respect to the length of the oligomer, thus there is little difference in the first association, whereas the second step is significantly affected. The  $k_2$  values increase and the  $k_{-2}$  values decrease of the *A. niger* wild-type glucoamylase with increasing substrate length. This means that the activation energy of the second step is less and is more easily overcome the longer is the substrate (at least up to five units of glucose), which has been shown also to account for the wild-type *Rhizopus* enzyme (Hiromi et al., 1983). This is significantly changed in the Trp120→Phe mutant reactions, where the chain length dependence of  $k_2$  for the formation of the mutant enzyme-substrate intermediate is opposite to that of the wild-type, and the  $k_2$  values decrease with increasing substrate length. Consequently, the activation energies of the second step are greater and more difficult to overcome the longer is the substrate. Thus, regarding the second reaction step, the mutation introduces a significant loss of assistance during the conformational change of the enzyme. With respect to  $K_2$  the intermediate wild-type enzyme-substrate complexes formed in the second reaction step are significantly more stable, the longer is the substrate, whereas the intermediate mutant enzyme-substrate complexes show a weaker tendency to this. Furthermore, the equilibrium of the second step is more shifted toward the intermediate in each of the mutant reactions than in the corresponding ones of the wild-type. Since the  $K_1$  values differ only slightly, what has been said with respect to  $K_2$  is also true of the overall dissociation constant,  $K_D$ , and of  $K_m$ .

When a Trp residue involved in the process is removed, as in Trp120→Phe, the signal,  $\Delta F_{\text{max}}(G_x, \infty)$ , is expected to change from that of wild-type. In the present case the observed change is a loss of the order of 12–20%. The smallest change is seen with maltose, the binding of which is also least affected by the mutation. Other Trp residues than Trp120 obviously play a role. This is known also from glucoamylase activity studies (Clarke & Svensson, 1984a,b; Svensson et al., 1986; Itoh et al., 1989; Sierks et al., 1989, 1993). The three-dimensional structure of the native form of a closely related enzyme (Aleshin et al., 1992) indicated several Trp residues located near the general acid group, Glu179, including Trp52, Trp178, Trp317, and Trp417. These may be particularly important in the enzyme-substrate complex formed in the second reaction step. Preliminary analysis of selected mutants has shown that of these Trp52 makes a dominant contribution to the quenching of the wild-type glucoamylase fluorescence (T. Christensen, K. Olsen, U. Christensen, and B. Svensson, unpublished data). Trp52 seems thus particularly important in the enzyme-substrate complex formed in the second reaction step, since no change of the intrinsic fluorescence is seen in

connection with the first association reaction neither in the wild-type nor the Trp120→Phe mutant. Since Trp52, like Trp120, has been found to hydrogen-bond to Glu179, the general acid catalyst (Aleshin et al., 1992), it is expected that conformational changes can be monitored in the wild-type as well as the Trp120→Phe glucoamylase. Trp120 previously has been assigned a role in communication between substrate glucosyl residues and the enzyme at subsites 2 and 4 (Clarke & Svensson, 1984a,b; Sierks et al., 1989; Svensson & Sierks, 1992). With respect to subsite 2, the interaction with maltose shows a weak effect of the mutation Trp120→Phe on the first association complex; that of the wild-type enzyme is a little more stable than that of the mutant ( $K_{1,wt} \leq K_{1,mu}$ ), whereas the effect on the enzyme–substrate intermediate formed in the second reaction step is larger and results in a mutant intermediate more stable than the wild-type intermediate ( $K_{2,wt} > K_{2,mu}$ ). This means that the line of departure, energetically speaking, for the actual catalytic step is less favorable in the mutant intermediate. The effects on the second reaction step, in contrast, are seen only in oligomers longer than maltose ( $k_{2,wt} > k_{2,mu}$ ) and are thus probably due to subsite 3 or 4 interactions.

This is in agreement with Trp120 being localized to a subsite at a distance from the catalytic site. The binding mechanism has not been studied in similar details for mutants of related carbohydrases. In *Saccharomyces*  $\alpha$ -amylase Trp82 is homologous to Trp83 in Taka-amylase A, which in turn resembles Trp120 in function and is found in a short region of very similar amino acid sequence (Clarke & Svensson, 1984b; Matsuura et al., 1984). Mutation of Trp82 of *Saccharomyces*  $\alpha$ -amylase leads to slow glycon product release resulting in oligomerization through transglycosylation (Matsui et al., 1991). This enzyme differs in the mechanism of action, however, since  $\alpha$ -amylases are retaining endo-acting hydrolases [for reviews, see Sinnott (1990) and Svensson and Søgaard (1993)]. Moreover, the catalytic domain is a ( $\beta/\alpha$ )<sub>8</sub>-barrel (Matsuura et al., 1984) and thus completely different from the ( $\alpha/\alpha$ )<sub>6</sub>-barrel fold found in glucoamylase (Aleshin et al., 1992).

Another significant effect of the Trp120→Phe mutation is on the rate-determining catalytic step of the reactions. As is expected,  $k_c$  of the *A. niger* wild-type enzyme (Meagher et al., 1989) like that of the wild-type *Rhizopus* enzyme (Hiromi et al., 1983) increases with the substrate length (13-fold) and also  $k_c$  of the mutant enzyme increases (6-fold), but the actual values of the mutant are approximately  $1/30$ – $1/80$  compared with those of the wild-type. In other terms the mutation leads to an approximate 8 kJ/mol increase of the transition state energy barrier, in agreement with a  $\Delta\Delta G^\ddagger$  of 10 kJ/mol for maltose and maltoheptaose hydrolysis at 50 °C between wild-type and Trp120→Phe mutant (Sierks et al., 1989).

As seen from our results (Table I), interactions at subsites 3, 4, and 5 reveal themselves not in the association complex but practically only in the second intermediate, which is the predominant species under steady-state conditions, to which the assignment of subsite binding energy contributions has been made. In these second intermediates the binding energy is provided mainly from interaction at subsite 2, and no or very little binding energy is provided from interactions at subsite 1 (Hiromi et al., 1983; Sierks et al., 1989). Reaction models previously suggested (Hiromi et al., 1983; Fagerström, 1991) parallel Scheme I as far as the number of steps are concerned. The values of the actual kinetic parameters determined here, however, presumably contradict the essence of these hypotheses. Subsite 2 may be predominantly

responsible but then cannot be fully utilized in the interactions of the first weak enzyme–substrate association complex ( $K_1$ ). Additional interactions at subsite 1 obviously cannot account for the binding energy observed of the intermediates formed in the second reaction step ( $K_1K_2$ ).

The kinetic studies performed here with acarbose describe its interaction with a carbohydrase in great details. It is interesting that the reaction mechanism of the binding of acarbose to glucoamylase apparently involves the same number of steps as the interactions of substrates with the enzyme (Figures 5 and 7) and that the first and the second reaction steps closely resemble those of the maltotetraose reaction, whereas the third step, which parallels the catalytic step of the substrate reactions, is the one in which the inhibitory nature of acarbose reveals itself. Acarbose is a tight-binding inhibitor of glucoamylase and has been referred to as a transition state analogue inhibitor. Thus, it is not surprising, that the final complex gives rise to a unique change of intrinsic fluorescence of the enzyme. But we find it interesting that two reaction steps apparently similar to those of the substrate binding precede the unique binding step of acarbose. If the structure of the enzyme is complementary to that of the transition state analogue inhibitor, only a single reaction step is expected. Now, a simple assignment of acarbose as a transition state analogue inhibitor is probably not reasonable, since the planar conformation in the valienamine moiety of acarbose differs from the expected planarity at C-1 of a sugar ring in the half-chair conformation during catalysis, because the double bond in this ring is between carbon atoms analogous to the ring oxygen and C-5 of a glucose ring (Truscheit et al., 1981; Bock & Pedersen, 1984). This may explain the changes seen here prior to the final binding step. Some structural changes in the enzyme apparently are necessary before the acarbose can be suitably accommodated. This seems important, since it means that neither the structure of the free enzyme nor that of the final complex need to be good representatives of the structure of the enzyme–substrate intermediate in which the actual catalytic step occurs.

Although it is difficult to discern the second the the third step of the acarbose-Trp120→Phe glucoamylase reaction (Figure 6), since the mutation leads to a significant decrease of  $k_2$  and at the same time an increase (approximately two orders of magnitude) of  $k_3$ , it seems highly likely that Scheme I also accounts for this reaction. In any case, the acarbose mutant intermediate formed before the unique (third) step shows weak binding ( $K_d' \approx 2$  mM) compared with that of maltotetraose ( $K_d \approx 5$   $\mu$ M) (Table II) or those either of acarbose or maltotetraose to the wild-type enzyme (Table I). Here again a role of Trp120 in the binding process of glucoamylase reveals itself. This residue seems much more important in the acarbose intermediate than in the substrate intermediates. This reflects a rather tight Trp120–acarbose interaction in the intermediate complex of the wild-type enzyme. It further indicates that the enzyme–substrate intermediates formed in the second reaction step are not structurally equivalent to the corresponding acarbose intermediate in spite of similar  $\Delta F_{max}(G_x, \infty)$  and  $K_d$  values (Table I). The fast third step of the formation of the acarbose mutant complex is partly explained by weak interactions in the preceding mutant intermediate, less bond breaking and rearrangements are needed compared with those of the acarbose wild-type complex.

#### ACKNOWLEDGMENT

Sidsel Ehlers is acknowledged for performing the steady-state kinetic experiments, and Dorte Boelskifte and Bjarne

Stoffer are acknowledged for purification of the glucoamylase Trp120→Phe mutant enzyme.

## REFERENCES

- Aleshin, A., Golubev, A., Firsov, L. M., & Honzatko, R. B. (1992) *J. Biol. Chem.* 267, 19291–19298.
- Bock, K., & Pedersen, H. (1984) *Carbohydr. Res.* 132, 142–149.
- Cherlinski, G. H. (1966) in *Chemical Relaxation*, pp 11–12, Marcel Dekker Inc., New York.
- Clarke, A. J., & Svensson, B. (1984a) *Carlsberg Res. Commun.* 49, 111–122.
- Clarke, A. J., & Svensson, B. (1984b) *Carlsberg Res. Commun.* 49, 559–566.
- Fleming, I. D., & Pegler, H. F. (1963) *Analyst* 88, 167–169.
- Fox, J. D., & Robyt, J. F. (1991) *Anal. Biochem.* 195, 93–96.
- Frandsen, T. P., Lehmbeck, J., Dupont, C., Stoffer, B., Sierks, M. R., Hansen, M. T., & Svensson, B. (1993) *Proc. 6th Eur. Congr. Biotechnol.*, Firenze, June 1993 (submitted).
- Harris, E. M. S., Aleshin, A. E., Firsov, L. M., & Honzatko, R. B. (1993) *Biochemistry* 32, 1618–1626.
- Hiromi, K., Takahashi, K., Hamauzu, Z., & Ono, S. (1966a) *J. Biochem. (Tokyo)* 59, 469–475.
- Hiromi, K., Kawai, M., & Ono, S. (1966b) *J. Biochem. (Tokyo)* 59, 476–480.
- Hiromi, K., Ohnishi, M., & Tanaka, A. (1983) *Mol. Cell Biochem.* 51, 79–95.
- Itoh, T., Ohtsuki, I., Yamashita, I., & Fukui, S. (1987) *J. Bacteriol.* 169, 4171–4176.
- Itoh, T., Sakata, Y., Akada, R., Nimi, O., & Yamashita, I. (1989) *Agric. Biol. Chem.* 53, 3159–3167.
- Kuriki, T., Takata, H., Okada, S., & Imanaka, T. (1991) *J. Bacteriol.* 173, 6147–6152.
- Martineau, P., Szmecman, S., Spurlino, J. C., Quirocho, F. A., & Hofnung, M. (1990) *J. Mol. Biol.* 214, 337–352.
- Matsui, I., Ishikawa, K., Miyari, S., Fukui, S., & Honda, K. (1991) *Biophys. Acta* 1077, 416–419.
- Matsuura, Y., Kusunoki, M., Harada, W., & Kakudo, M. (1984) *J. Biochem. (Tokyo)* 95, 697–702.
- Meagher, M. M., Nikolov, Z. L., & Reilly, P. J. (1989) *Biotech. Bioeng.* 34, 681–688.
- Nagashima, T., Toda, S., Kitamoto, K., Gomi, K., Kumagai, C., & Toda, H. (1992) *Biosci. Biotech. Biochem.* 56, 207–210.
- Nakamura, A., Haga, K., Ogawa, S., Kuwano, K., Kimura, K., & Yamane, K. (1992) *FEBS Lett.* 296, 37–40.
- Ohnishi, M., Matsumoto, T., Yamanaka, T., & Hiromi, K. (1990) *Carbohydr. Res.* 204, 187–196.
- Olsen, K., Svensson, B., & Christensen, U. (1992) *Eur. J. Biochem.* 209, 777–784.
- Savel'ev, A. N., & Firsov, L. M. (1983) *Biokhimiya* 48, 1125–1132.
- Sierks, M. R., Ford, C., Reilly, P. J., & Svensson, B. (1989) *Protein Eng.* 2, 621–625.
- Sierks, M. R., Ford, C., Reilly, P. J., & Svensson, B. (1990) *Protein Eng.* 3, 193–198.
- Sierks, M. R., Ford, C., Reilly, P. J., & Svensson, B. (1993) *Protein Eng.* 6, 75–79.
- Sinnott, M. L. (1990) *Chem. Rev.* 90, 1171–1202.
- Stoffer, B., Frandsen, T. P., Busk, P. K., Schneider, P., Svendsen, I., & Svensson, B. (1993) *Biochem. J.* 292, 197–203.
- Svensson, B., & Sierks, M. R. (1992) *Carbohydr. Res.* 227, 29–44.
- Svensson, B., & Søgaard, M. (1993) *J. Biotechnol.* 29, 1–37.
- Svensson, B., Pedersen, T. G., Svendsen, I., Sakai, T., & Ottesen, M. (1982) *Carlsberg Res. Commun.* 47, 55–69.
- Svensson, B., Clarke, A. J., & Svendsen, I. (1986) *Carlsberg Res. Commun.* 51, 61–73.
- Svensson, B., Clarke, A. J., Svendsen, I., & Møller, M. (1990) *Eur. J. Biochem.* 188, 29–38.
- Tanaka, A., Ohnishi, M., & Hiromi, K. (1982) *Biochemistry* 21, 107–113.
- Truscheit, E., Frommer, W., Junge, B., Müller, L., Schmidt, D. D., & Wingender, W. (1981) *Angew. Chem.* 93, 738–755.